Chapter 5

Ultrasound Measuring of Porosity in Porous Materials

Zine El Abiddine Fellah, Mohamed Fellah,
Claude Depollier, Erick Ogam and Farid G. Mitri

Additional information is available at the end of the chapter

http://dx.doi.org/10.5772/intechopen.72696

Abstract

This chapter provides a temporal method for measuring the porosity and the tortuosity of air-saturated porous materials using experimental reflected waves. The direct problem of reflection and transmission of acoustic waves by a slab of porous material is studied. The equivalent fluid model has considered in which the acoustic wave propagates only in the pore-space. Since the acoustic damping in air-saturated porous materials is important, only the reflected waves by the first interface are taken into account, and the multiple reflections are neglected. The study of the sensitivity analysis shows that porosity is much more sensitive than tortuosity to reflection, especially when the incident angle is less than its critical value, at which the reflection coefficient vanishes. The inverse problem is solved using experimental data at a different incidence angle in reflection. Some advantages and perspectives of this method are discussed.

Keywords: porosity, tortuosity, porous material

1. Introduction

Porosity [1–3] is one of the most important parameters for describing the acoustic propagation in porous materials. This parameter intervenes in the propagation phenomena at all frequencies. Porosity is the relative fraction, by volume, of the air contained within the material. Air-saturated porous materials [1, 2, 4] as plastic foams, fibrous or granular materials are of great interest for a wide range of industrial applications. **Figure 1** gives an example of air-saturated porous material commonly used in the sound absorption (passive control). These materials are frequently used in the automotive and aeronautics industries and in the building trade. Beranek [3] has developed an apparatus for measuring the porosity of air saturated porous materials. This device was based on the equation of state for ideal gases at constant temperature i.e., Boyle's law. Porosity can be determined by measuring the change in air pressure occurring with a known change in volume of the chamber containing the sample. In this apparatus, both

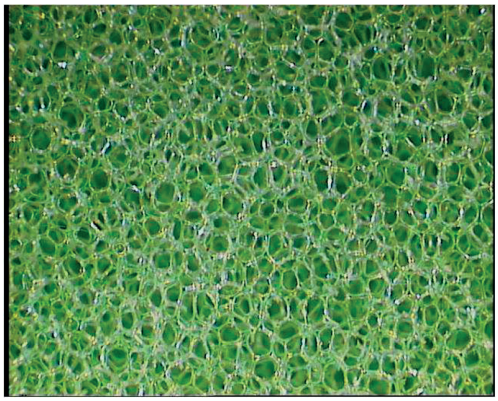

Figure 1. Air saturated plastic foam.

pressure change and volume change are monitored using a U-shaped fluid-filled manometer. Leonard [6] has given an alternate dynamic method for measuring porosity. Other techniques using water as the pore-filling fluid, rather than air, are common in geophysical studies [7, 8]. Mercury has been used as the pore-filling fluid in other applications [9]. However, for many materials, the introduction of liquids into the material is not appropriate. Recently, a similar device to that of Beranek [3], involving the use of an electronic pressure transducer, was introduced by Champoux et al. [10]. This device can be used to measure very slight changes in pressure accurately, and the output can be recorded by a computer.

Generally, the most methods used for measuring the porosity cited previously do not use acoustic waves. Here, we present an ultrasonic method for measuring porosity using ultrasonic reflected waves by the porous material. The direct and inverse problem is solved in the time domain using experimental reflected data. The inverse problem is solved directly in time domain using the waveforms. The attractive feature of a time domain-based approach [11–16] is that the analysis is naturally limited by the finite duration of ultrasonic pressures and is consequently the most appropriate approach for the transient signal.

2. Model

In the acoustics of porous materials, a distinction can be made between two situations depending on whether the frame is moving or not. In the general case (when the frame is moving), as for cancellous bone and rock and all porous media saturated by a liquid, the dynamics of the waves due to the coupling between the solid frame and the fluid are clearly described by the Biot theory [17, 18]. In air-saturated porous media, as plastic foams or fibrous materials that are used in sound absorption, the structure is generally motionless and the waves propagate only in the fluid. This case is described by the model of equivalent fluid, which is a particular case in the Biot model, in which the interactions between the fluid and the structure are taken into account in two frequency response factors: the dynamic tortuosity of the medium

$\alpha(\omega)$ given by Johnson et al. [4] and the dynamic compressibility of the air included in the porous material $\beta(\omega)$ given by Allard and Champoux [5]. In the frequency domain, these factors multiply the density of the fluid and its compressibility, respectively, and represent the deviation from the behavior of the fluid in free space as the frequency increases. In the time domain, they act as operators, and in the high-frequency approximation, their expressions are given by [11]

$$\tilde{\alpha}(t) = \alpha_\infty \left(\delta(t) + \frac{2}{\Lambda} \left(\frac{\eta}{\pi \rho_f} \right)^{1/2} t^{-1/2} \right), \tag{1}$$

$$\tilde{\beta}(t) = \left(\delta(t) + \frac{2(\gamma - 1)}{\Lambda'} \left(\frac{\eta}{\pi Pr \rho_f} \right)^{1/2} t^{-1/2} \right). \tag{2}$$

In these equations, $\delta(t)$ is the Dirac function, Pr is the Prandtl number, η and ρ_f are fluid viscosity and fluid density, respectively, and γ is the adiabatic constant. The most important physical parameters of the model are the medium's tortuosity α_∞ initially introduced by Zwikker and Kosten [2] and viscous and the thermal characteristic lengths Λ and Λ' introduced by Johnson et al. [4] and Allard and Champoux [5]. In this model, the time convolution of $t^{-1/2}$ with a function is interpreted as a semi-derivative operator according to the definition of the fractional derivative of order ν given in Samko et al. [19]

$$D^\nu[x(t)] = \frac{1}{\Gamma(-\nu)} \int_0^t (t-u)^{-\nu-1} x(u) du, \tag{3}$$

where $\Gamma(x)$ is the Gamma function.

In this framework, the basic equations of our model can be expressed as follows

$$\rho_f \tilde{\alpha}(t) * \frac{\partial v_i}{\partial t} = -\nabla_i p \quad \text{and} \quad \frac{\tilde{\beta}(t)}{K_a} * \frac{\partial p}{\partial t} = -\nabla . v, \tag{4}$$

where $*$ denotes the time convolution operation, p is the acoustic pressure, v is the particle velocity and K_a is the bulk modulus of the air. The first equation is the Euler equation, the second is a constitutive equation obtained from the equation of mass conservation associated with the behavior (or adiabatic) equation.

In the plane (xoz), the constitutive equation (4) can be written as

$$\begin{aligned}
\rho_f \alpha_\infty \frac{\partial v_x(x,z,t)}{\partial t} + \frac{2\rho_f \alpha_\infty}{\Lambda} \left(\frac{\eta}{\pi \rho_f} \right)^{1/2} \int_0^t \frac{\partial v_x(x,z,t')/\partial t'}{\sqrt{t-t'}} dt' &= -\frac{\partial p(x,z,t)}{\partial x}, \\
\rho_f \alpha_\infty \frac{\partial v_z(x,z,t)}{\partial t} + \frac{2\rho_f \alpha_\infty}{\Lambda} \left(\frac{\eta}{\pi \rho_f} \right)^{1/2} \int_0^t \frac{\partial v_z(x,z,t')/\partial t'}{\sqrt{t-t'}} dt' &= -\frac{\partial p(x,z,t)}{\partial z}, \\
\frac{1}{K_a} \frac{\partial p(x,z,t)}{\partial t} + \frac{2(\gamma-1)}{K_a \Lambda'} \left(\frac{\eta}{\pi \rho_f P_r} \right)^{1/2} \int_0^t \frac{\partial p(x,z,t')/\partial t'}{\sqrt{t-t'}} dt' &= -\frac{\partial v_x(x,z,t)}{\partial x} - \frac{\partial v_z(x,z,t)}{\partial z},
\end{aligned} \tag{5}$$

where v_x and v_z are the components of particle velocity along axes x and z. In these equations, the integrals express the fractional derivatives, defined mathematically by convolutions and describe the dispersive nature of the porous material. They take into account the memory effects due to the fluid-structure interactions and to the viscous and thermal losses in the medium.

The problem geometry is shown in **Figure 2**. A homogeneous porous material occupies the region $0 \le x \le L$. This medium is assumed to be isotropic and to have a rigid frame. A short sound pulse impinges at oblique incidence on the medium from the left, giving rise to an acoustic pressure field $p(x,z,t)$ and an acoustic velocity field $\mathbf{v}(x,z,t)$ within the material, which satisfies the system of Eq. (5) that can be written as:

$$\rho_f \alpha_\infty \frac{\partial v_x(x,z,t)}{\partial t} + \frac{2\rho_f \alpha_\infty}{\Lambda}\left(\frac{\eta}{\rho_f}\right)^{1/2} D^{1/2}[v_x(x,z,t)] = -\frac{\partial p(x,z,t)}{\partial x}, \tag{6}$$

$$\rho_f \alpha_\infty \frac{\partial v_z(x,z,t)}{\partial t} + \frac{2\rho_f \alpha_\infty}{\Lambda}\left(\frac{\eta}{\rho_f}\right)^{1/2} D^{1/2}[v_z(x,z,t)] = -\frac{\partial p(x,z,t)}{\partial z}, \tag{7}$$

$$\frac{1}{K_a}\frac{\partial p(x,z,t)}{\partial t} + \frac{2(\gamma-1)}{K_a \Lambda'}\left(\frac{\eta}{\rho_f P_r}\right)^{1/2} D^{1/2}[p(x,z,t)] = -\frac{\partial v_x(x,z,t)}{\partial x} - \frac{\partial v_z(x,z,t)}{\partial z}. \tag{8}$$

In the region $x \le 0$, the incident pressure wave is given by

$$p^i(x,z,t) = p^i\left(t - \frac{x\cos\theta}{c_0} - \frac{z\sin\theta}{c_0}\right), \tag{9}$$

where c_0 is the velocity of the free fluid ($x \le 0$); $c_0 = \sqrt{K_a/\rho_f}$.

In the region $0 \le x \le L$, the pressure wave is given by

$$p(x,z,t) = p\left(t - \frac{x\cos\theta'}{c'} - \frac{z\sin\theta'}{c'}\right), \tag{10}$$

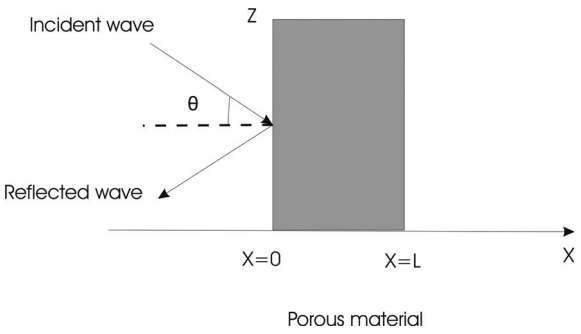

Figure 2. Problem geometry.

where c' is the velocity in the porous material ($0 \le x \le L$), and the refraction angle θ' is given by the Descartes-Snell law [27, 28]:

$$\frac{\sin\theta}{c_0} = \frac{\sin\theta'}{c'} \tag{11}$$

To simplify the system of Eq. (5), we can then use the following property

$$\frac{\partial}{\partial z} = -\frac{\sin\theta}{c_0}\frac{\partial}{\partial t}, \tag{12}$$

which implies

$$\frac{\partial v_z}{\partial z} = -\frac{\sin\theta}{c_0}\frac{\partial v_z}{\partial t} \quad \text{and} \quad \frac{\partial p}{\partial z} = -\frac{\sin\theta}{c_0}\frac{\partial p}{\partial t}. \tag{13}$$

From Eqs. (7) and (13), we obtain the relation

$$\frac{\partial v_z}{\partial z} = -\frac{\sin^2\theta}{c_0^2}\left(\rho_f\alpha_\infty + \frac{2\rho_f\alpha_\infty}{\Lambda}\left(\frac{\eta}{\rho_f}\right)^{1/2} D^{-1/2}\right)^{-1} * \frac{\partial p}{\partial t}. \tag{14}$$

By using Eqs. (6), (8) and (14), the equation systems (6), (7) and (8) can thus be simplified to

$$\rho_f\alpha_\infty\frac{\partial v_x(x,z,t)}{\partial t} + \frac{2\rho_f\alpha_\infty}{\Lambda}\left(\frac{\eta}{\rho_f}\right)^{1/2} D^{1/2}[v_x(x,z,t)] = -\frac{\partial p(x,z,t)}{\partial x}, \tag{15}$$

$$\begin{aligned}&\frac{1}{K_a}\frac{\partial p(x,z,t)}{\partial t} + \frac{2(\gamma-1)}{K_a\Lambda'}\left(\frac{\eta}{\rho_f P_r}\right)^{1/2} D^{1/2}[p(x,z,t)] = \\ &-\frac{\partial v_x(x,z,t)}{\partial x} + \frac{\sin^2\theta}{c_0^2}\left(\rho_f\alpha_\infty + \frac{2\rho_f\alpha_\infty}{\Lambda}\left(\frac{\eta}{\rho_f}\right)^{1/2} D^{-1/2}\right)^{-1} * \frac{\partial p(x,z,t)}{\partial t}.\end{aligned} \tag{16}$$

From Eqs. (15) and (16), we derive the fractional propagation wave equation in the time domain along the x-axis

$$\frac{\partial^2 p(x,z,t)}{\partial x^2} - \frac{1}{c_0^2}\left(\alpha_\infty - \sin^2\theta\right)\frac{\partial^2 p(x,z,t)}{\partial t^2} - \frac{2\alpha_\infty}{K_a}\sqrt{\frac{\rho_f\eta}{\pi}}\left(\frac{1}{\Lambda} + \frac{\gamma-1}{\sqrt{\mathrm{Pr}}\Lambda'}\right)D^{3/2}[p(x,z,t)] = 0, \tag{17}$$

The solution of the wave Eq. (17) with suitable initial and boundary conditions is by using the Laplace transform. F is the medium's Green function [12, 20] given by

$$F(t,k) = \begin{cases} 0 & \text{if} \quad 0 \le t \le k \\ \Xi(t) + \Delta\int_0^{t-k} h(t,\xi)d\xi & \text{if} \quad t \ge k \end{cases} \tag{18}$$

with

$$\Xi(t) = \frac{b'}{4\sqrt{\pi}} \frac{k}{(t-k)^{3/2}} \exp\left(-\frac{b'^2 k^2}{16(t-k)}\right), \tag{19}$$

where $h(\tau, \xi)$ has the following form:

$$h(\xi, \tau) = -\frac{1}{4\pi^{3/2}} \frac{1}{\sqrt{(\tau-\xi)^2 - k^2}} \frac{1}{\xi^{3/2}} \int_{-1}^{1} \exp\left(-\frac{\chi(\mu, \tau, \xi)}{2}\right) (\chi(\mu, \tau, \xi) - 1) \frac{\mu d\mu}{\sqrt{1-\mu^2}} \tag{20}$$

and $\chi(\mu, \tau, \xi) = \left(\Delta\mu\sqrt{(\tau-\xi)^2 - k^2} + b'(\tau-\xi)\right)^2 / 8\xi$, $b' = Bc_0^2\sqrt{\pi}$ and $\Delta = b'^2$.

If the incident sound wave is launched in region $x \leq 0$, then the expression of the pressure field in the region on the left of the material is the sum of the incident and reflected fields

$$p_1(x, t, \theta) = p^i\left(t - \frac{x\cos\theta}{c_0}\right) + p^r\left(t + \frac{x\cos\theta}{c_0}\right), \qquad x < 0. \tag{21}$$

Here, $p_1(x, t, \theta)$ is the field in the region $x < 0$, p^i and p^r denote the incident and reflected fields, respectively.

The incident and reflected fields are related by the scattering operator (i.e., the reflection operator) for the material. This is an integral operator represented by

$$p^r(x, t, \theta) = \int_0^t \tilde{R}(\tau, \theta) p^i\left(t - \tau + \frac{x\cos\theta}{c_0}\right) d\tau, \tag{22}$$

In Eq. (22), the function $\tilde{R}$ is the reflection kernel for incidence from the left. Note that the lower limit of integration in Eq. (22) is set to 0, which is equivalent to assuming that the incident wavefront impinges on the material at $t = 0$.

Expression of the reflection-scattering operator taking into account the n-multiple reflections in the material is given by

$$\tilde{R}(t, \theta) = \left(\frac{1-E}{1+E}\right) \sum_{n \geq 0} \left(\frac{1-E}{1+E}\right)^{2n} \left[F\left(t, 2n\frac{L}{c}\right) - F\left(t, (2n+2)\frac{L}{c}\right)\right], \tag{23}$$

with

$$E = \frac{\phi\sqrt{1 - \frac{\sin^2\theta}{\alpha_\infty}}}{\sqrt{\alpha_\infty}\cos\theta}, \tag{24}$$

Generally [21], in air-saturated porous materials, acoustic damping is very important, and the multiple reflections are thus negligible inside the material. So, by taking into account only

the first reflections at interfaces $x = 0$ and $x = L$, the expression of the reflection operator will be given by

$$\tilde{R}(t,\theta) = r(t,\theta) + \mathfrak{R}(t,\theta), \tag{25}$$

with

$$r(t,\theta) = \left(\frac{1-E}{1+E}\right)\delta(t) \quad \text{and} \quad \mathfrak{R}(t,\theta) = -\frac{4E(1-E)}{(1+E)^3}F\left(t,\frac{2L}{c}\right), \tag{26}$$

where $r(t,\theta)$ is the instantaneous response of the porous material corresponding to the reflection contribution at the first interface ($x = 0$). $\mathfrak{R}(t,\theta)$ is equivalent to reflection at the interface $x = L$, which is the bulk contribution to reflection. The part of the wave corresponding to $r(t,\theta)$ is not subjected to dispersion but simply multiplied by the factor $(1-E)/(1+E)$.

The reflection coefficient at the first interface vanishes for a critical angle θ_c

$$r(t,\theta) = 0 \Rightarrow \sin\theta_c = \sqrt{\frac{\alpha_\infty(\alpha_\infty - \phi^2)}{\alpha_\infty^2 - \phi^2}}.$$

Figure 3 shows the variation of the reflection coefficient at the first interface r with the incident angle θ, for a fixed porosity value $\phi = 0.9$, and for different values of tortuosity $\alpha_\infty = 1.99$ (solid line), $\alpha_\infty = 1.75$ (star), $\alpha_\infty = 1.5$ (dashed line), $\alpha_\infty = 1.24$ (dash-dot line) and $\alpha_\infty = 1$ (circle).

Figure 4 shows the variation of r with the incident angle, for a fixed tortuosity of $\alpha_\infty = 1.1$, and for different values of porosity $\phi = 0.99$ (solid line), $\phi = 0.75$ (star), $\phi = 0.50$ (dashed line), $\phi = 0.25$ (dash-dot line) and $\phi = 0.01$ (circle).

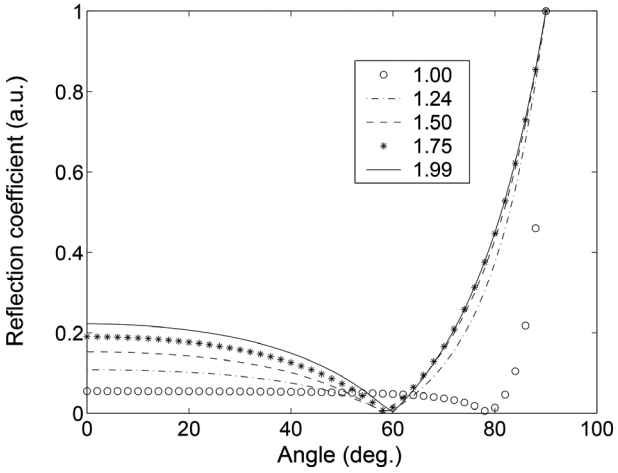

Figure 3. Variation of the reflection coefficient at the first interface r with the incident angle θ, for a fixed porosity value $\phi = 0.9$, and for different values of tortuosity $\alpha_\infty = 1.99$ (solid line), $\alpha_\infty = 1.75$ (star), $\alpha_\infty = 1.5$ (dashed line), $\alpha_\infty = 1.24$ (dash-dot line) and $\alpha_\infty = 1$ (circle).

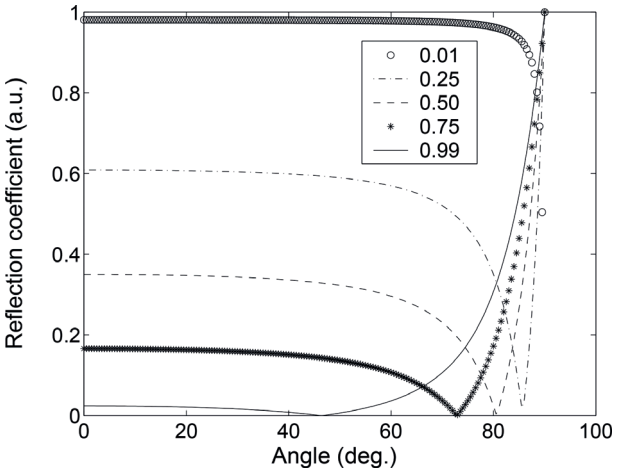

Figure 4. Variation of the reflection coefficient at the first interface with the incident angle, for a fixed tortuosity value $\alpha_\infty = 1.1$, and for different values of porosity $\phi = 0.99$ (solid line), $\phi = 0.75$ (star), $\phi = 0.50$ (dashed line), $\phi = 0.25$ (dash-dot line) and $\phi = 0.01$ (circle).

When the incident angle is $\theta < \theta_c$, the reflection coefficient decreases slowly with the incident angle, and when it is $\theta > \theta_c$, the reflection coefficient increases quickly with the angle. It can be seen also from **Figures 2** and **3** that the sensitivity of porosity variation is more important than the sensitivity of tortuosity on the reflection coefficient at the first interface.

3. Inverse problem

The inverse problem is solved using transmitted waves and an estimation of the tortuosity, viscous and thermal characteristic length is given. However, the porosity cannot be inverted in transmission since its sensitivity is low. In this work, we determine porosity and tortuosity by solving the inverse problem for waves reflected by the first interface and by taking into account experimental data concerning all measured incident angles (**Figure 4**). The propagation of acoustic waves in a slab of porous material in the high-frequency asymptotic domain is characterized by four parameters: porosity ϕ, tortuosity α_∞, viscous characteristic length Λ, and thermal characteristic length Λ', the values of which are crucial to the behavior of sound waves in such materials. It is of some importance to work out new experimental methods and efficient tools for their estimation. The basic inverse problem associated with the slab may be stated as follows: from the measurement of the signals transmitted and/or reflected outside the slab, find the values of the medium's parameters. The inverse problem is to find values of parameters ϕ, α_∞, which minimize the function:

$$U(\phi, \alpha_\infty) = \sum_{\theta_i} \sum_{t_i} \left[p^r(x, \theta_i, t_i) - r(\theta_i, t_i) * p^i(x, \theta_i, t_i) \right]^2, \tag{27}$$

where $p^r(x, \theta_i, t_i)$ represents the discrete set of values of the experimental reflected signal for different incident angles θ_i, $r(\theta_i, t_i)$ is the reflection coefficient at the first interface, and $p^i(x, \theta_i, t_i)$ is the experimental incident signal. The term $r(\theta_i, t_i) * p^i(x, \theta_i, t_i)$ represents the predicted reflected signal. The inverse problem is solved numerically by the least-square method.

Let us consider three samples of plastic foam M1, M2, and M3. Their tortuosity and porosity were measured using classical methods [22–31] (**Table 1**). We solved the inverse problem for these samples via waves reflected at the first interface and for different incident angles.

Experiments were performed in air with two broadband Ultran NCT202 transducers with a 190 kHz central frequency in air and a 6 dB bandwidth extending from 150 to 230 kHz. Pulses of 400 V were provided by a 5052PR panametrics pulser/receiver. An optical goniometer was used to position the transducers. The received signals were amplified to 90 dB and filtered above 1 MHz to avoid high-frequency noise. Electronic interference was removed by 1000 acquisition averages. The experimental setup is shown in **Figure 5**.

Figures 6 and **7** show a variation of the cost function, U, with tortuosity and porosity, for samples M1, M2, and M3, respectively. The reconstructed values of porosity and tortuosity corresponding to the positions of the minima of these cost functions are given in **Table 2**.

Material	M1	M2	M3
Tortuosity	1.1	1.1	1.5
Porosity	0.95	0.99	0.86

Table 1. Measured values of porosity and tortuosity by classical methods [22–31].

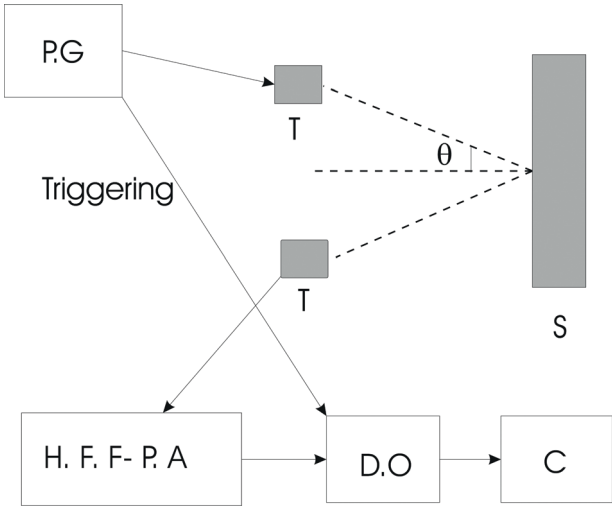

Figure 5. Experimental set-up of the ultrasonic measurements in reflected mode. PG: pulse generator; HFFPA: high-frequency filtering-pre-amplifier; DO: digital oscilloscope; C: computer; T: transducer; S: sample.

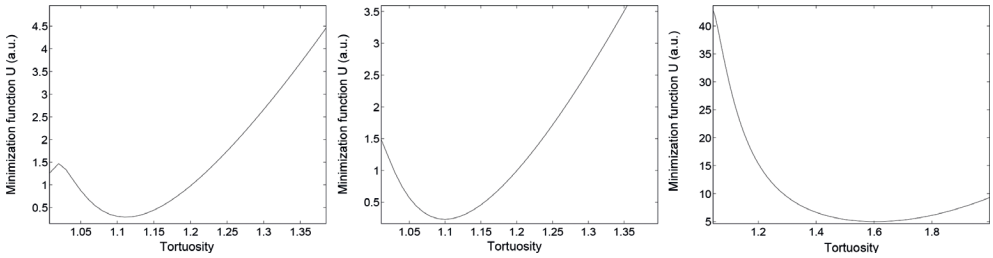

Figure 6. Variation of the cost function *U* with tortuosity for the plastic foams M1, M2, and M3.

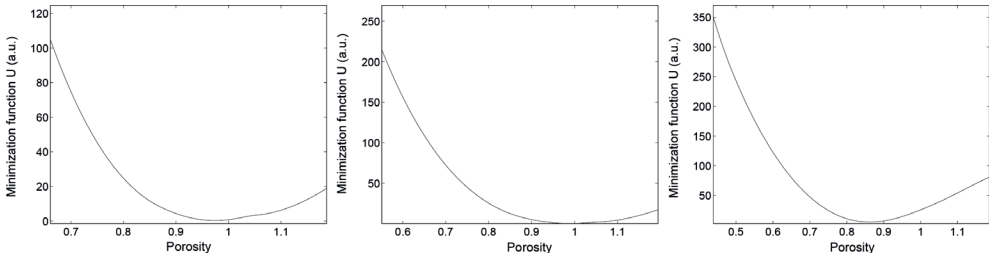

Figure 7. Variation of the cost function *U* with porosity for the plastic foams M1, M2, and M3.

Material	M1	M2	M3
Tortuosity	1.12	1.1	1.6
Porosity	0.96	0.99	0.85

Table 2. Reconstructed values of porosity and tortuosity by solving the inverse problem.

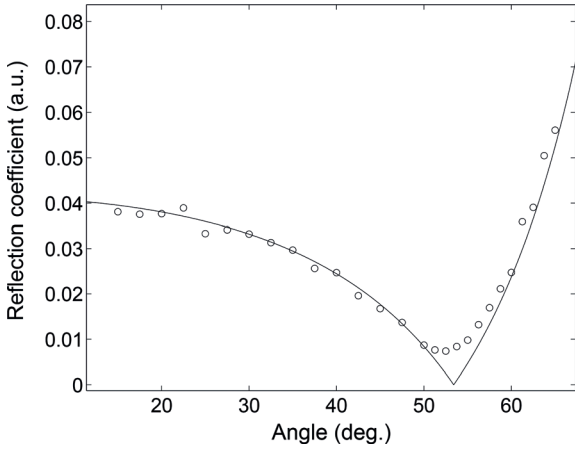

Figure 8. Comparison between simulated reflection coefficient at the first interface using reconstructed values of the porosity and tortuosity (solid line) and experimental data of the reflection coefficient at the first interface (circle) for the plastic foam M1.

A comparison is given in **Figures 8–10**, between simulated reflection coefficient at the first interface using reconstructed values of porosity and tortuosity (solid line) and experimental data of the reflection coefficient at the first interface (circle) for plastic foams M1, M2, and M3, respectively.

The correspondence between experiment and theory is good, which leads us to conclude that this method based on the solution of the inverse problem is appropriate for estimating the porosity and tortuosity of porous materials with a rigid frame. This method is very interesting comparing the classical one using non-acoustic waves.

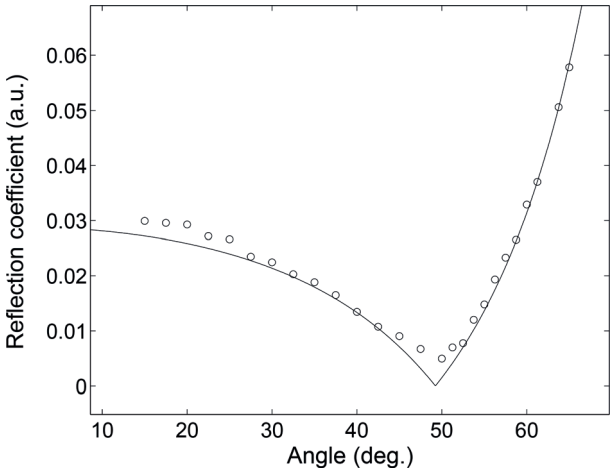

Figure 9. Comparison between simulated reflection coefficient at the first interface using reconstructed values of the porosity and tortuosity (solid line) and experimental data of the reflection coefficient at the first interface (circle) for the plastic foam M2.

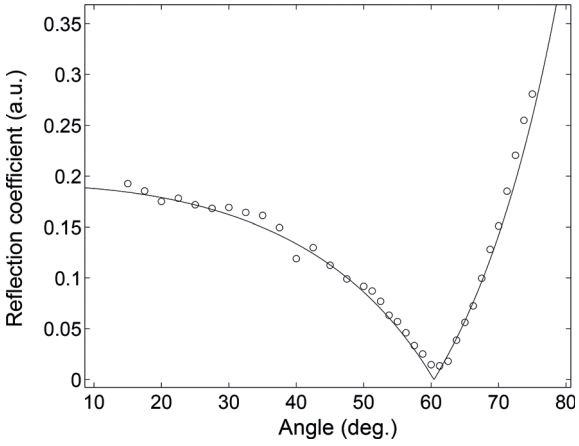

Figure 10. Comparison between simulated reflection coefficient at the first interface using reconstructed values of the porosity and tortuosity (solid line) and experimental data of the reflection coefficient at the first interface (circle) for the plastic foam M3.

4. Conclusion

In this chapter, an inverse determination of porosity and tortuosity is given using experimental reflected acoustic waves at different incidence angles. The inverse problem is solved numerically by the least-square method. The obtained values of porosity and tortuosity are close to those given using classical (non-acoustical) methods. Generally, the tortuosity is inverted easily using transmitted waves, and this is not the case for porosity because of its weak sensitivity in transmitted mode. This method is very interesting from its simplicity and constitutes an alternative to the usual method involving the use of a porosimeter introduced by Beranek [3] and improved by Champoux et al. [10] or the other ultrasonic methods based on transmitted mode.

This method is valuable for porous materials having a rigid frame as air-saturated media, in which the equivalent fluid model is used. However, for liquid-saturated materials as rock or cancellous bone, this method cannot be used and should be adapted using the general Biot model [17, 18]. We hope, in the future, to extend this method to porous media with an elastic frame saturated with viscous fluid, in order to estimate other parameters that play an important role in acoustic propagation.

Author details

Zine El Abiddine Fellah[1]*, Mohamed Fellah[2], Claude Depollier[3], Erick Ogam[1] and Farid G. Mitri[4]

*Address all correspondence to: fellah@lma.cnrs-mrs.fr

1 LMA, CNRS, UPR 7051, Aix-Marseille Univ, Centrale Marseille, Marseille Cedex 20, France

2 Laboratoire de Physique Théorique, Faculté de Physique, USTHB, Bab-Ezzouar, Algeria

3 LUNAM Universite du Maine, UMR CNRS 6613 Laboratoire d'Acoustique de l'Universite du Maine, Cedex 09, France

4 Chevron, Santa Fe, New Mexico, United States

References

[1] Allard JF. Propagation of Sound in Porous Media: Modeling Sound Absorbing Materials. London: Chapman and Hall; 1993

[2] Zwikker C, Kosten CW. Sound Absorbing Materials. New York: Elsevier; 1949

[3] Beranek LL. Acoustic impedance of porous materials. The Journal of the Acoustical Society of America. 1942;**13**:248-260

[4] Johnson DL, Koplik J, Dashen R. Theory of dynamic permeability and tortuosity in fluid-saturated porous media. Journal of Fluid Mechanics. 1987;**176**:379-402

[5] Allard JF, Champoux Y. New empirical equations for sound propagation in rigid frame fibrous materials. Acoustical Society of America. 1992;**91**:3346

[6] Leonard RW. Simplified porosity measurements. Journal of the Acoustical Society of America. 1948;**20**:39-34

[7] Guyon E, Oger L, Plona TJ. Transport properties in sintered porous media composed of two particles sizes. Journal of Physics D: Applied Physics. 1987;**20**:1637-1644

[8] Johnson DL, Plona TJ, Scala C, Psierb F, Kojima H. Tortuosity and acoustic slow waves. Physical Review Letters. 1982;**49**:1840-1844

[9] Van Brakel J, Modry S, Svata M. Mercury porosimetry: State of the art. Powder Technology. 1981;**29**:1-12

[10] Champoux Y, Stinson MR, Daigle GA. Air-based system for the measurement of porosity. The Journal of the Acoustical Society of America. 1991;**89**:910-916

[11] Fellah ZEA, Depollier C. Transient acoustic wave propagation in rigid porous media: A time domain approach. Journal of the Acoustical Society of America. 2000;**107**(2):683-688

[12] Fellah ZEA, Depollier C, Fellah M, Lauriks W, Chpaleon JY. Influence of dynamic tortuosity and compressibility on the propagation of transient waves in porous media. Wave Motion. 2005;**41**(2):145-161

[13] Fellah ZEA, Fellah M, Lauriks W, Depollier C. Direct inverse scattering of transient acoustic waves by a slab of rigid porous material. Journal of the Acoustical Society of America. 2003;**113**(1):61-72

[14] Szabo TL. Time domain wave equations for lossy media obeying a frequency power law. The Journal of the Acoustical Society of America. 1994;**96**:491

[15] Szabo TL. Causal theories and data for acoustic attenuation obeying a frequency power law. Journal of the Acoustical Society of America. 1995;**97**:14

[16] Norton V, Novarini JC. Including dispersion and attenuation directly in time domain for wave propagation in isotropic media. The Journal of the Acoustical Society of America. 2003;**113**:3024

[17] Biot MA. The theory of propagation of elastic waves in fluid-saturated porous solid. I. Low frequency range. The Journal of the Acoustical Society of America. 1956;**28**:168

[18] Biot MA. The theory of propagation of elastic waves in fluid-saturated porous solid. I. Higher frequency range. The Journal of the Acoustical Society of America. 1956;**28**:179

[19] Samko SG, Kilbas AA, Marichev OI. Fractional Integrals and Derivatives Theory and Applications. Amsterdam: Gordon and Breach Publishers; 1993

[20] Fellah ZEA, Fellah M, Lauriks W, Depollier C, Angel Y, Chapelon JY. Solution in time domain of ultrasonic propagation equation in porous material. Wave Motion. 2003;**38**: 151-163

[21] Fellah ZEA, Mitri FG, Depollier C, Berger S, Lauriks W, Chapelon JY. Characterization of porous materials with a rigid frame via reflected waves. Journal of Applied Physics. 2003;**94**:7914-7922

[22] Fellah ZEA, Ogam E, Wirgin A, Fellah M, Depollier C, Lauriks W. Ultrasonic characterization of porous materials: Inverse problem. Journal of Sound and Vibration. 2007;**302**: 746-759

[23] Leclaire P, Kelders L, Lauriks W, Glorieux C, Thoen J. Determination of the viscous characteristic length in air-filled porous materials by ultrasonic attenuation measurements. The Journal of the Acoustical Society of America. 1996;**99**:1944

[24] Leclaire P, Kelders L, Lauriks W, Brown NR, Melon M, Castagnède B. Determination of viscous and thermal characteristic lengths of plastic foams by ultrasonic measurements in helium and air. Journal of Applied Physics. 1996;**80**:2009

[25] Fellah ZEA, Depollier C, Berger S, Lauriks W, Trompette P, Chapelon JY. Detemination of transport parameters in air saturated porous materials via ultrasonic reflected waves. The Journal of the Acoustical Society of America. 2003;**113**(5):2561-2569

[26] Fellah ZEA, Berger S, Lauriks W, Depollier C, Chapelon JY. Inverse problem in air-saturated porous media via reflected waves. Review of Scientific Instruments. 2003;**74**(5): 2871

[27] Fellah ZEA, Berger S, Lauriks W, Depollier C, Aristégui C, Chapelon JY. Measuring the porosity and the tortuosity of porous materials via reflected waves at oblique incidence. The Journal of the Acoustical Society of America. 2003;**113**(5):2424

[28] Fellah ZEA, Berger S, Lauriks W, Depollier C, Trompette P, Chapelon JY. Ultrasonic measuring of the porosity and tortuosity of air- saturated random packings of beads. Journal of Applied Physics. 2003;**93**:9352

[29] Fellah ZEA, Mitri FG, Depollier D, Berger S, Lauriks W, Chapelon JY. Characterization of porous materials having a rigid frame via reflected waves. Journal of Applied Physics. 2003;**94**:7914

[30] Fellah ZEA, Berger S, Lauriks W, Depollier C, Fellah M. Measurement of the porosity of porous materials having a rigid frame via reflected waves: A time domain analysis with fractional derivatives. Journal of Applied Physics. 2003;**93**:296

[31] Fellah ZEA, Mitri FG, Fellah M, Ogam E, Depollier C. Ultrasonic characterization of porous absorbing materials: Inverse problem. Journal of Sound and Vibration. 2007;**302**: 746-759